Reactivity of $LiBH_4$: In Situ Synchrotron Radiation Powder X-ray Diffraction Study

Lene Mosegaard,[†] Bitten Møller,[†] Jens-Erik Jørgensen,[†] Yaroslav Filinchuk,[‡] Yngve Cerenius,[§] Jonathan C. Hanson,[||] Elaine Dimasi,[⊥] Flemming Besenbacher,[#] and Torben R. Jensen*[,†]

Interdisciplinary Nanoscience Center (iNANO) and Department of Chemistry, University of Aarhus, Langelandsgade 140, DK-8000 Aarhus C, Denmark, SNBL at ESRF, 6 rue Jules Horowitz, 38043 Grenoble Cedex, France, MAX-lab, Lund University, S-22100 Lund, Sweden, Chemistry Department, Brookhaven National Laboratory, Upton, New York 11973, National Synchrotron Light Source Department, Brookhaven National Laboratory, Upton, New York 11973, and Interdisciplinary Nanoscience Center (iNANO) and Department of Physics and Astronomy, University of Aarhus, Ny Munkegade, 8000 Aarhus C, Denmark

Received: August 31, 2007; In Final Form: October 29, 2007

Lithium tetrahydridoboranate ($LiBH_4$) may be a potentially interesting material for hydrogen storage, but in order to absorb and desorb hydrogen routinely and reversibly, the kinetics and thermodynamics need to be improved significantly. A priori, this material has one of the highest theoretical gravimetric hydrogen contents, 18.5 wt %, but unfortunately for practical applications, hydrogen release occurs at too high temperature in a non-reversible way. By means of in situ synchrotron radiation powder X-ray diffraction (SR-PXD), the interaction between $LiBH_4$ and different additives—SiO_2, $TiCl_3$, LiCl, and Au—is investigated. It is found that silicon dioxide reacts with molten $LiBH_4$ and forms Li_2SiO_3 or Li_4SiO_4 at relatively low amounts of SiO_2, e.g., with 5.0 and 9.9 mol % SiO_2 in $LiBH_4$, whereas, for higher amounts of SiO_2 (e.g., 25.5 mol %), only the Li_2SiO_3 phase is observed. Furthermore, we demonstrate that a solid-state reaction occurs between $LiBH_4$ and $TiCl_3$ to form LiCl at room temperature. At elevated temperatures, more LiCl is formed simultaneously with a decrease in the diffracted intensity from $TiCl_3$. Lithium chloride shows some solubility in solid $LiBH_4$ at $T > 100$ °C. This is the first report of substituents that accommodate the structure of $LiBH_4$ by a solid/solid dissolution reaction. Gold is found to react with molten $LiBH_4$ forming a Li−Au alloy with $CuAu_3$-type structure. These studies demonstrate that molten $LiBH_4$ has a high reactivity, and finding a catalyst for this H-rich system may be a challenge.

Introduction

Recently, there has been increased focus on sustainable and renewable energy sources as alternatives to the present use of fossil fuels. Many of these energy outputs are, however, not constant in time, and therefore there is huge interest in developing an efficient, robust, rechargeable energy storage system. Hydrogen is considered an interesting energy carrier for the future, and the storage of hydrogen in hydride materials may be a safe, efficient, and cheap way for mobile applications, such as cars and trucks, but a number of both fundamental and more technological challenging issues still have to be solved before the proposed hydrogen society can become a reality.[1−4]

Solid-state storage of hydrogen as a metal hydride is studied intensively and is currently considered to be one of the most promising routes to reach high storage capacities in the future. Most of the proposed hydrogen storage materials have high volumetric hydrogen densities, up to 150 g H_2/L for Mg_2FeH_6, which is more than twice the density of liquid hydrogen, 71 g H_2/L.[5] To achieve high gravimetric hydrogen densities, one needs to focus on the light metals, e.g., Li, Na, Mg, B, and Al, and these are known to form a variety of metal hydride materials.[6−9]

A potentially interesting material is the complex metal hydride $LiBH_4$, which contains a large amount of hydrogen, measured by both mass and volume (18.5 wt % and 121 g H_2/L), but unfortunately the hydrogen release occurs at too high temperatures in a non-reversible way for practical applications. A modification of this system, e.g., by adding a catalyst, is therefore called upon, and this has prompted us to study this material further. The structure of $LiBH_4$ is built from tetrahedra of BH_4^- and Li^+ ions, each having a coordination number of four. Normally, $LiBH_4$ exists as an orthorhombic phase at low temperatures and transforms to a hexagonal phase at approximately 108 °C, and these two phases are denoted *o*- and *h*-$LiBH_4$, respectively.[10,11] It is found that $LiBH_4$ releases hydrogen in several steps; a hydrogen release of ca. 1 wt % has been observed at 380 °C, followed by a main desorption of ca. 9 wt % H_2, in the temperature range 420−600 °C.[11] Powder diffraction patterns of two new phases were observed during the decomposition of $LiBH_4$, but their detailed structures and composition remain unknown.[12] Furthermore, several new structures and compositions of lithium tetrahydridoboranates were proposed from theoretical calculations.[13−15] In order to release more hydrogen reversibly at lower temperatures, further knowledge of the mechanism of gas release is needed. Alter-

* Corresponding author. E-mail address: trj@chem.au.dk. Address: Interdisciplinary Nanoscience Center (iNANO), Department of Chemistry, University of Aarhus, Langelandsgade 140, DK-8000 Aarhus C, Denmark. Phone: +45 8942 3894. Fax: +45 8619 6199.

[†] Interdisciplinary Nanoscience Center (iNANO) and Department of Chemistry, University of Aarhus.

[‡] SNBL at ESRF.

[§] Lund University.

[||] Chemistry Department, Brookhaven National Laboratory.

[⊥] National Synchrotron Light Source Department, Brookhaven National Laboratory.

[#] Interdisciplinary Nanoscience Center (iNANO) and Department of Physics and Astronomy, University of Aarhus.

10.1021/jp076999v CCC: $40.75
Published on Web 01/09/2008 PAGE EST: 4.9

natively, a catalyst can be added or a new reaction pathway can be obtained from a suitable reactive hydride composite. The latter can be achieved using a relatively large amount of another hydride as additive, which may shift the thermodynamics of the reaction to lower temperatures.[16−18] In contrast, only a small amount of a catalytic additive is necessary in order to enhance the kinetics of the process. Pure $LiBH_4$ is known to decompose to lithium hydride and boron, releasing 13.6 wt % H_2 at an equilibrium temperature of $T = 410$ °C ($p(H_2) = 1$ bar) corresponding to $\Delta H = -68.9$ kJ/mol H_2.[19] On the other hand, the reactive composite hydride $LiBH_4/MgH_2$ (2:1) releases 11.5 wt % H_2 reversible during the formation of LiH and MgB_2 at an equilibrium temperature of $T = 168$ °C ($p(H_2) = 1$ bar), corresponding to $\Delta H = 45.8$ kJ/mol H_2.[20,21] Furthermore, a mixture of $LiNH_2$ and $LiBH_4$ (2:1) also releases hydrogen at moderate conditions (10 wt % at ca. 250 °C) and involves the formation of a quaternary hydride, $Li_4(BH_4)(NH_2)_3$, containing an ordered arrangement of BH_4^- and NH_2^- ions.[22,23] The kinetics of hydrogen release and uptake can be catalyzed by metals, oxides or chlorides of the transition metals in some cases. The interaction of $LiBH_4$ with different selected additives (Au, SiO_2, LiCl and $TiCl_3$) is therefore further investigated in this study using in situ synchrotron radiation powder X-ray diffraction (SR-PXD) in order to improve the hydrogen storage properties of this promising material.

Experimental Section

Sample Preparation. Samples of $LiBH_4$ with different additives, i.e., Au, SiO_2, LiCl, or $TiCl_3$, were investigated. Silicon dioxide (SiO_2, cristobalite) (5.0, 9.9, or 25.5 mol %) was added to $LiBH_4$ and crushed for ca. 5 min by hand in an agate mortar and afterward blended for ca. 10 min with a ball grinder using 10 glass balls (0.5 mm o.d.). Samples of $LiBH_4$ containing $TiCl_3$ (2.0 mol %) or Au (1.8, 1.5, or 0.29 mol %) were crushed in an agate mortar for ca. 10 min by hand in order to obtain a homogeneous mixture. Samples of $LiBH_4$ containing 15 mol % LiCl were ball-milled 60 times in 2 min intervals separated by 2 min pauses. The speed of the main disk was 200 rounds per minute, and the speed of the planets was −560 rounds per minute using a Fritsch pulverisette no. 4. The sample-to-ball ratio was 1:156 using a WC vessel and 10 mm WC balls. As a standard, 5 wt % Au was added to the ball-milled $LiBH_4$ and LiCl sample, and the mixture was crushed in an agate mortar for ca. 10 min by hand to obtain a homogeneous mixture. An overview of the experimental work is provided in Table 1. The chemicals used were $LiBH_4$ (95%, Aldrich), SiO_2, cristobalite (purified and calcined, Merck), $TiCl_3$ (99.999%, Aldrich), and Au powder (spherical, < 5 μm, 99.95%, Alfa Aesar). Dry LiCl was prepared from $LiCl{\cdot}H_2O$ (Aldrich, %) kept at 120 °C for 5 days. All handling and manipulation of the chemicals were performed in an argon-filled glove box.

In Situ Time-Resolved (SR-PXD). Data were collected at the synchrotron NSLS, Brookhaven National Laboratory beamlines X7B and X6B, and at the synchrotron MAX II, Lund, Sweden, MAX-Lab beamline I711 with a MAR345 image plate (X7B), a Simens CCD area detector (X6B), and a MAR165 CCD detector (I711) system.[24,25] The selected wavelengths were in the range of 0.65255−1.1072 Å. The sample cell was specially developed for studies of gas/solid reactions and allows high pressure and temperature to be applied.[26,27] The samples were mounted in a sapphire single-crystal tube (1.09 mm o.d., 0.79 mm i.d., Al_2O_3) in an argon-filled glove box ($p(O_2, H_2O) < 0.3$ ppm). The temperature was controlled with a thermocouple placed in the sapphire tube next to the sample. A gas supply system was attached to the sample cell, which allowed the change of gas and pressure via a vacuum pump during X-ray data acquisition. The system was flushed with N_2 or He (see Table 1) and evacuated three times before the valve to the sample was opened prior to the X-ray experiment. The X-ray exposure time was 30−60 s per powder diffraction pattern. The FIT2D program was used to remove diffraction spots from the sapphire sample holder and to transform raw data to powder patterns.[28]

TABLE 1: Experimental Details for the In Situ SR-PXD Experiments Performed with $LiBH_4$ and Additives[a]

		thermal treatment	
sample no.	additive (mol %)	T_{max} (°C)	$\Delta T/\Delta t$ (°C/min)
1	0	600	3.2
	$LiBH_4 + SiO_2$		
2	5.0	400	5.0
3	5.0	500	5.0
4	5.0	500	3.0
5	9.9	500	5.0
6	9.9	500	3.0
7	25.5	500	3.0
8	25.5	500	3.0
9	25.5	500	5.0
	$LiBH_4 + Au$		
10	1.5	600	4.7
11	1.8	400	5.0
12	0.3	400	4.8
	$LiBH_4 + TiCl_3$		
13	2.0	300	5.0
	$LiBH_4 + LiCl$		
14	15	250	5.0

[a] The samples were heated from RT to T_{max} with a fixed heating rate, $\Delta T/\Delta t$.

Sample Characterization. In-house powder X-ray diffraction (PXD) data was measured in Debye−Scherrer geometry using a Stoe diffractometer equipped with a curved Ge (111) monochromator (Cu Kα_1 radiation, $\lambda = 1.54060$ Å) and a curved position-sensitive detector covering 28°. Air-sensitive samples measured at room temperature (RT) were mounted between two thin (3.6 μm) Mylar films. Samples for high-temperature measurements were mounted in a quartz capillary (0.5 mm i.d.) in an argon-filled glove box and sealed with epoxy glue prior to the experiments. The sample was heated 5 °C/min to fixed temperatures of 30, 50, 70, and 90 °C + $n{\cdot}10$ °C ($n = 1, 2 \ldots 16$) where PXD data was collected from 16 to 43° in 2θ with a counting time of 420 s. The program Origin 6.1 was used to perform a numerical integration of selected diffraction peaks for each phase for estimation of the sample composition at different temperatures. The following reflections were used: *o*-$LiBH_4$: (101), (011), (200) (002); *h*-$LiBH_4$: (100), (002), (101); LiCl: (111), (200); and Au: (111).

Differential thermal analysis was performed using a Netzsch STA449C Jupiter instrument (heating rate 10 °C/min, RT to 330 °C) and aluminum oxide crucibles with lids as sample holders. The phase transformation from *o*- to *h*-$LiBH_4$ and the melting point of $LiBH_4$ were observed at 112 ± 2 °C and 281 ± 2 °C, respectively, for all samples (temperatures are measured as the onset of the thermal event). These data were used as an internal temperature calibration for the in situ SR-PXD experiments.

Results and Discussion

In the following, the interaction between $LiBH_4$ and different additives is investigated, and in order to minimize possible

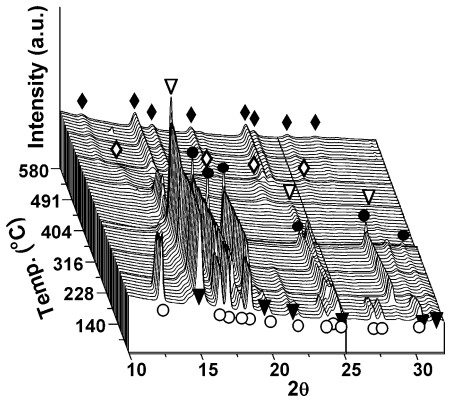

Figure 1. Series of SR-PXD patterns for a $LiBH_4$ mixture with 5 mol % SiO_2 heated from RT to 580 °C (Table 1, sample no. 2) showing the formation of crystalline silicates (5 °C/min, $\lambda = 1.06218$ Å). Symbols: ○ *o*-$LiBH_4$, ● *h*-$LiBH_4$, ▼ SiO_2 (tetragonal), ▽ SiO_2 (cubic), ◇ Li_2SiO_3, and ◆ Li_4SiO_4.

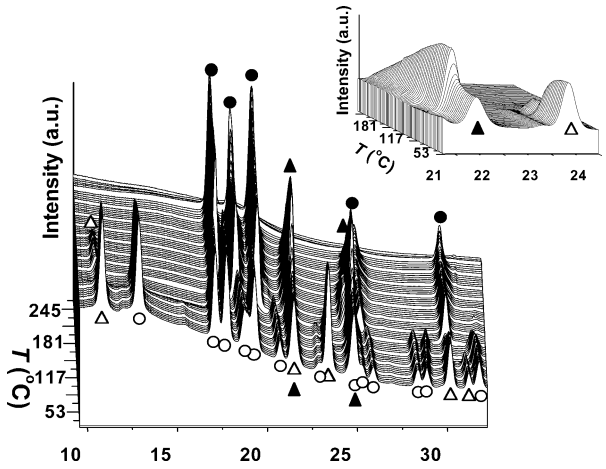

Figure 2. SR-PXD patterns from $LiBH_4$ with 2 mol % $TiCl_3$ heated from RT to 300 °C showing the formation of LiCl already at RT (sample no. 13, see Table 1) (5 °C/min, $\lambda = 1.1072$ Å). The inset shows the increase in the intensity of LiCl peaks simultaneously with a decrease in the intensity of the peaks from $TiCl_3$. Symbols: ○ *o*-$LiBH_4$, ● *h*-$LiBH_4$, ▲ LiCl, and △ $TiCl_3$.

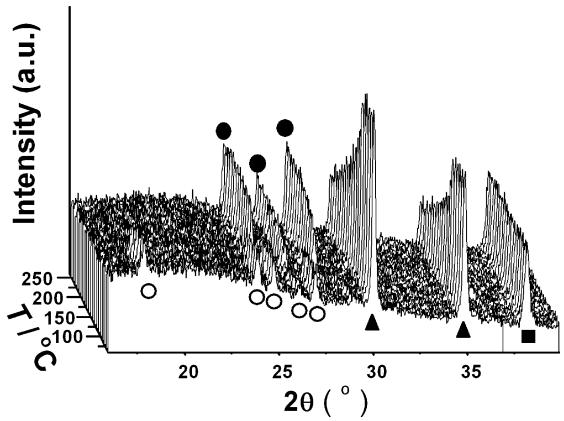

Figure 3. PXD patterns from $LiBH_4$ with 15 mol % LiCl heated from RT to 250 °C showing a decrease in the diffracted intensity of LiCl at ca. 120 °C, simultaneously with an increase in the diffracted intensity of $LiBH_4$. (5 °C/min, $\lambda = 1.54060$ Å) Symbols: ○ *o*-$LiBH_4$, ● *h*-$LiBH_4$, ▲ LiCl, and ■ Au.

reactions prior to experimental investigation, the reactants were only mixed in a mortar.

Silicon Dioxide as Additive in $LiBH_4$. A possible catalytic effect of SiO_2 on the dehydrogenation of $LiBH_4$ was previously reported, but the exact reaction mechanism remains unknown.[11] In order to investigate the interaction between lithium tetrahydridoboranate and silicon dioxide, several samples with different molar ratios (see Table 1) were studied using in situ SR-PXD. Data that is broadly representative of the results for the SiO_2 additive is presented in the following.

A series of in situ SR-PXD patterns measured for a sample of $LiBH_4$ mixed with 5 mol % SiO_2 is shown in Figure 1. Reflections in the powder patterns from RT to 110 °C can be indexed as orthorhombic $LiBH_4$ (*o*-$LiBH_4$) and tetragonal SiO_2 (cristobalite) with the following refined unit cell parameters: $a = 7.243(11)$, $b = 4.460(6)$, $c = 6.892(9)$ Å and $a = 5.027(9)$, $c = 7.065(16)$ Å, respectively, both refined at $T = 50$ °C.[11,29] Cristobalite (SiO_2) transforms to a cubic structure in the temperature range 200−370 °C, $a = 7.178(7)$ Å at $T = 327$ °C. The hexagonal high-temperature phase of $LiBH_4$ (*h*-$LiBH_4$) was observed from 110 to 280 °C, where the sample melted. In the temperature range 220−285 °C, weak reflections (not shown in Figure 1) were observed, which correspond to the new hexagonal variant of partly dehydrogenated lithium tetrahydridoboranate, denoted as phase I.[12] SiO_2 was the only crystalline phase observed in the temperature range from 275 to 370 °C. In all experiments with different amounts of the additive SiO_2, the formation of lithium metasilicate (Li_2SiO_3) was verified at ca. 370 °C. By adding less than 10 mol % SiO_2 to $LiBH_4$, the orthosilicate (Li_4SiO_4) was observed at ca. 450 °C, but its formation was not noticed using 25 mol % SiO_2. Apparently, Li needs to be in excess to facilitate the formation of the orthosilicate Li_4SiO_4. In earlier studies, the hydrogen release (13.5 wt % at $200 < T < 600$ °C) from $LiBH_4$ containing glass powder (25 wt % $LiBH_4$ and 75 wt % glass powder) was seen at $T > 200$ °C, which is at lower temperatures than that for pure $LiBH_4$.[11] Our studies demonstrate that an irreversible reaction between molten $LiBH_4$ and SiO_2 occurs.

$LiBH_4$ Mixed with $TiCl_3$. Titanium trichloride has a well-documented catalytic effect on the hydrogen release and uptake from $NaAlH_4$.[30] Furthermore, earlier studies have demonstrated that $TiCl_3$ lowers the hydrogen desorption temperature of $LiBH_4$, and this prompted the present study.[31]

It was initially noticed that the color of a sample of $LiBH_4$ with 2 mol % $TiCl_3$ changed from light red/purple to gray/black when kept a few hours at RT in an argon-filled glove box, which indicates that a chemical reaction takes place. The chemical reaction causing the color change can be suppressed when the sample is instead kept at low temperatures, $T = -35$ °C. The reaction between $LiBH_4$ and $TiCl_3$ was studied for 20 h at RT with PXD, and the formation of LiCl was clearly observed (data not shown). In situ SR-PXD data recorded from a similar sample of $LiBH_4$ with 2 mol % of $TiCl_3$ is displayed in Figure 2 (see Table 1, sample 13) and clearly demonstrates that $TiCl_3$ partly reacts with $LiBH_4$ to form LiCl already at RT prior to the X-ray experiment.

The inset in Figure 2 shows that the diffracted intensity from $TiCl_3$ is almost constant in the temperature range from RT to 50 °C, but decreases at higher temperatures and disappears at 177 °C. The diffracted intensity from LiCl is also almost constant in the temperature range from RT to 50 °C, but then increases to a maximum at $T = 85$ °C. Surprisingly, the diffracted intensity from LiCl decreases in the temperature range from 100 to 245 °C. This was further investigated by in situ PXD of a sample containing $LiBH_4$ ball-milled with 15 mol % LiCl heated from RT to 250 °C, as shown in Figure 3. This sample was ball-milled to bring the solids in intimate contact and to study possible solid-state reactions at temperatures below

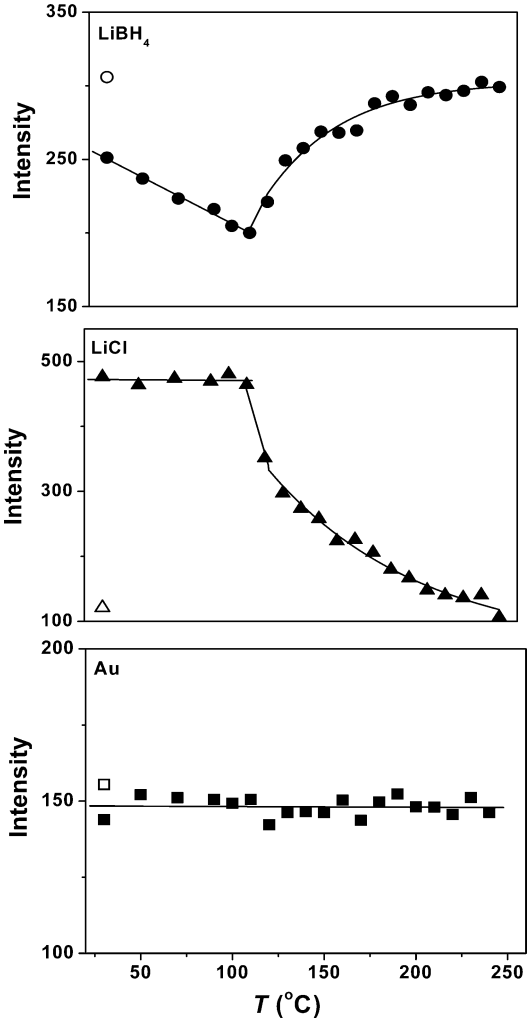

Figure 4. Integrated diffracted intensity of selected reflections from $LiBH_4$, LiCl, and Au shown as a function of temperature. It is found that LiCl is dissolved in the *h*-$LiBH_4$ structure at temperatures above 116 °C. Symbols: ● *h*-$LiBH_4$, ▲ LiCl, and ■ Au. (Open symbols are data measured after heating the sample.)

the melting point of $LiBH_4$. A decrease in the diffracted intensity of LiCl was observed above ca. 120 °C in the diffraction data, correlating with an increase in the diffracted intensity of $LiBH_4$. Figure 4 shows the integrated diffracted intensity of selected reflections from $LiBH_4$, LiCl, and Au as a function of temperature. The decrease in diffracted intensity from *o*-$LiBH_4$ in the temperature range from RT to 110 °C is possibly correlated with the increasing disorder as a result of the librational and reorientational motion of BH_4^- tetrahedra as the *o*- to *h*-$LiBH_4$ phase transition is approached.[32] At temperatures above 110 °C, the data clearly demonstrate the relationship between the increasing diffracted intensity of *h*-$LiBH_4$ and the disappearance of LiCl, which indicates that solid LiCl is dissolved in the structure of solid *h*-$LiBH_4$. This finding is rather unexpected because of the structural differences between wurtzite-type *h*-$LiBH_4$ (coordination number four) and the sodium chloride-type structure of LiCl (coordination number six). However, the cation−anion distances are similar in these two structures, being 2.57 and 2.80 Å for the Li−Cl and Li−B contacts, respectively. Extreme reorientational displacement motion around the trigonal axis of BH_4^- in *h*-$LiBH_4$ was recently observed by neutron vibrational spectroscopy and Raman spectroscopy.[32−34] As a result, *h*-$LiBH_4$ might have increased structural flexibility and reactivity, which might explain the dissolution of LiCl to some extent in the solid *h*-$LiBH_4$.

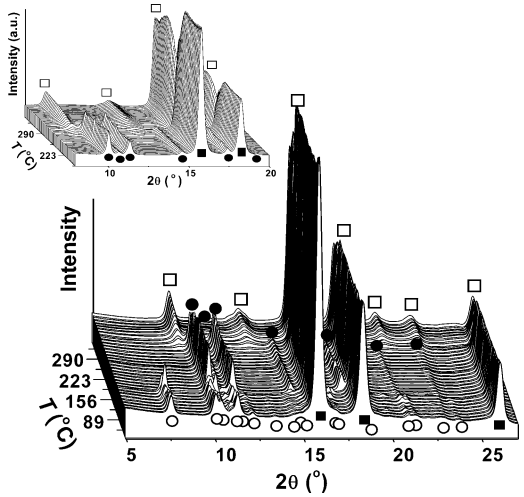

Figure 5. Stack of powder diffraction patterns from a sample of $LiBH_4$ with 1.5 mol % Au heated from RT to 340 °C (sample no. 11, see Table 1) (5 °C/min, $\lambda = 0.65255$ Å). It is observed that $LiBH_4$ reacts with Au after the melting point, and a new $AuCu_3$-type structure of Li and Au is formed. Symbols: ○ *o*-$LiBH_4$, ● *h*-$LiBH_4$, ■ Au, and □ Li_xAu_{1-x}.

It has previously been proposed that an ion-exchange reaction between of $LiBH_4$ and $TiCl_3$ resulting in LiCl and $Ti(BH_4)_3$ can occur, where $Ti(BH_4)_3$ decomposes and releases hydrogen at 25 °C and forms metallic borides.[35] Titanium or titanium borides were not observed in the PXD data, and the latter is possibly due to relatively high crystallization temperatures as compared to the temperatures used in this investigation. Earlier desorption measurements of ball-milled samples of $LiBH_4$ with ca. 4 mol % $TiCl_3$ showed no hydrogen release at temperatures above 100 °C.[31] This may indicate that a chemical reaction between $LiBH_4$ and $TiCl_3$ occurred already during ball-milling.

$LiBH_4$ Mixed with Au. Gold is a noble and inert metal, but, on the other hand, numerous recent studies have shown that Au nanoparticles are indeed very reactive and have interesting catalytic properties.[36] Therefore, it was decided to study the influence of Au utilized as an additive in $LiBH_4$.

In a previous study of intermediate phases obtained by heating $LiBH_4$, a gold foil was utilized as crucible. It was noticed that the gold foil obtained a darker color and that the white $LiBH_4$ powder was more foam-like and gained a harder surface, even though the heat treatment was performed below the melting point of $LiBH_4$.[12] This finding might indicate that a gold-catalyzed reaction occurred. In order to further study this phenomenon, $LiBH_4$ was mixed with gold powder (1.5 mol %) and examined by in situ SR-PXD, as shown in Figure 5. Prior to the melting point of $LiBH_4$, a significant decrease in the intensity of the diffraction peaks assigned to gold was observed (see inset in Figure 5). At the melting point of $LiBH_4$, a set of new reflections is observed, and these are assigned to a new Li−Au compound.

All diffraction peaks from the new phase were indexed with a cubic unit cell $a = 4.0614(5)$ Å. The $AuCu_3$-type structure with the space group $Pm3m$ has been utilized as a model, keeping the 1*a* Wyckoff site completely filled by Au atoms and refining the occupancy of the 3*c* Wyckoff site. Refinement converged at $R_B = 8.1\%$, $R_p = 3.6\%$, $R_{wp} = 5.55$, and 60.5(5)% occupation of the 3*c* site by Au atoms. A composition of the Li−Au alloy cannot be deduced on the basis of the site occupancies only, since we have to assume occupancy of at least one site. In this case the 1*a* site was assumed to be occupied by Au atoms only, though it may actually show a mixed Li and

Au occupation. The composition may be estimated from the refined unit cell parameter. Gold is expected to have the unit cell axis $a = 4.094$ Å at 365 °C,[37] which is slightly larger than the lattice parameter for the Li−Au alloy. On the other hand, a relatively Li-rich Li−Au alloy reveals ca. 8% volume contraction compared to that of pure Au.[38] These data thus suggest that the Li−Au alloy, obtained from the reaction between molten $LiBH_4$ and Au, is a Au-rich alloy.

It is interesting that the $AuCu_3$-type structure has been reported for the $LiAu_3$ compound.[38] However, while in this case for Li_xAu_{1-x} the 1*a* site is more rich in gold than 3*c*, in the $LiAu_3$ phase, the 1*a* site is occupied by Li atoms, and the 3*c* site is occupied by Au only. Although the Li−Au alloy is identified here as a partly ordered $AuCu_3$-type variant of the *F*-centered structure of Au, the real symmetry of the structure may be lower than the cubic observed as a small shift of superstructure peaks compared to their theoretical positions. These shifts can be well explained by the presence of staking faults.

During the reaction between molten $LiBH_4$ and Au, the formation of LiH might occur, but reflections from LiH are not observed in the diffraction data (Figure 5), possibly due to an overlap between reflections from the Li−Au alloy and LiH. No reflections from boron-containing phases are observed after the melting of $LiBH_4$, which might be due to the ability of boron to form glass phases.

Conclusion

An in situ PXD study has been performed with a focus on the reactions between $LiBH_4$ and different additives, i.e., SiO_2, $TiCl_3$, LiCl, and Au. It was found that quartz reacts with molten $LiBH_4$ in a irreversible manner and forms Li_2SiO_3, and, in mixtures with low amounts of SiO_2, the orthosilicate Li_4SiO_4 was also found. Therefore, hydrogen release from samples of $LiBH_4$ containing SiO_2 is likely due to a chemical reaction and not a catalytic process. It was also demonstrated that a solid-state reaction occurs at RT between $LiBH_4$ and $TiCl_3$ to form LiCl. Surprisingly, it is observed that LiCl is dissolved in the structure of solid *h*-$LiBH_4$ at temperatures above ca. 100 °C. This is the first example of a chemical substitution in $LiBH_4$. This may open a way to modify this H-rich system in order to improve its hydrogen storage properties. Gold reacts with molten $LiBH_4$, resulting in a new Li_xAu_{1-x} phase, which has a $CuAu_3$-type structure. These studies demonstrate that molten $LiBH_4$ has a high reactivity. Therefore, it is a challenge to find a material that could act as a catalyst for hydrogen release and uptake in $LiBH_4$ without being consumed in a chemical reaction with molten $LiBH_4$. On the other hand, the high reactivity can be a useful property, which may provide new reactive hydride composites, e.g., in analogy with the system $2LiBH_4 + MgH_2 \leftrightarrow MgB_2 + 2LiH + 4H_2$. The result presented here that additives can be accommodated in the structure of solid $LiBH_4$, as observed here for LiCl, may reveal an alternative synthetic route for new improved hydrogen storage materials based on lithium tetrahydridoboranate.

Acknowledgment. We thank the Danish Natural Science Research Council (DanSync program) and the Carlsberg Foundation for financial support. We are grateful to Brookhaven National Laboratory, supported under contract DE-AC02-98CH10886 with the U.S. Department of Energy by its Division of Chemical Sciences Office of Basic and Energy Sciences.

References and Notes

(1) Schlapbach, L.; Züttel, A. *Nature* **2001**, *414*, 353−358.
(2) Ritter, J. A; Ebner, A. D.; Wang, J.; Zidan, R. *Mater. Today* **2003**, *6*, 18−23.
(3) U.S. Department of Energy Home Page. http://www.eere.energy-.gov/hydrogenandfuelcells/hydrogen/-storage.html.
(4) Züttel, A. *Naturwissenschaften* **2004**, *91*, 157−172.
(5) Yvon, K.; Renaudin, G., In *Encyclopedia of Inorganic Chemistry*, 2nd ed.; John Wiley & Sons, Ltd.: New York, 2005; 1814−1846.
(6) Edwards, P. P.; David, W. I. F.; Jones, M. O.; Johnson, S. R.; Lowton, R. L.; Anderson, P. A.; Chater, P. A *Prepr. Pap. − Am. Chem. Soc., Div. Fuel Chem.* **2006**, *51* (2), 566.
(7) Dornheim, M.; Eigen, N.; Barkhordarian, G.; Klassen, T.; Bormann, R. *Adv. Eng. Mater.* **2006**, *8*, 377.
(8) Jensen, T. R.; Andreasen, A.; Vegge, T.; Andreasen, J. W.; Ståhl, K.; Pedersen, A. S.; Nielsen, M. M.; Molenbroek, A. M.; Besenbacher, F. *Int. J. Hydrogen Energy* **2006**, *31*, 2052−2062.
(9) Schüth, F.; Bogdanovic, B. and Felderhoff, M. *Chem. Commun.* **2004**, 2249−2258.
(10) Soulié, J.-Ph.; Renaudin, G.; Cerný, R.; Yvon, K. *J. Alloys Compd.* **2002**, *346*, 200−205.
(11) Züttel, A.; Rentsch, S.; Fischer, P.; Wenger, P.; Sudan, P.; Mauron, Ph.; Emmenegger, Ch. *J. Alloys Compd.* **2003**, *356−357*, 515−520.
(12) Mosegaard, L.; Møller, B.; Jørgensen, J.-E.; Bösenberg, U.; Dornheim, M.; Hanson, J. C.; Cerenius, Y.; Walker, G.; Jakobsen, H. J.; Besenbacher, F.; Jensen, T. R. *J. Alloys Compd.* **2007**, *446−447*, 301−305.
(13) Lodziana, Z.; Vegge, T. *Phys. Rev. Lett.* **2004**, *93*, 145501.
(14) Kang, J. K.; Kim, S. Y.; Han, Y. S.; Muller, R. P.; Goddard, W. A., III. *Appl. Phys. Lett.* **2005**, *87*, 111904.
(15) Ohba, N.; Miwa, K.; Aoki, M.; Noritake, T.; Towata, S.; Nakamori, Y.; Orimo, S.; Züttel, A. *Phys. Rev. B* **2006**, *74*, 075110.
(16) Barkhordarian, G.; Klassen, T.; Bormann, R. Pending German Patent 10 2004 061 286.2, 2004; Pending International Patent PCT/EP 2005/003494, 2005.
(17) Barkhordarian, G.; Klassen, T.; Dornheim, M.; Bormann, M. *J. Alloys Compd.* **2007**, *1−2*, L18−L21.
(18) Vajo, J. J.; Olson, G. L. *Scr. Mater.* **2007**, *56*, 829−834.
(19) Smith, M. B.; Brass, G. E., Jr. *J. Chem. Eng. Data* **1963**, *8*, 342.
(20) Bösenberg, U.; Doppiu, S.; Mosegaard, L.; Barkhordarian, G.; Eigen, N.; Borgschulte, A.; Jensen, T. R.; Cerenius, Y.; Gutfleisch, O.; Klassen, T.; Dornheim, M.; Borman, R. *Acta Mater.* **2007**, *55*, 3951−3958.
(21) Vajo, J. J.; Skeith, S. L.; Mertens, F. *J. Phys. Chem. B* **2005**, *109*, 3719.
(22) Pinkerton, F. E.; Meisner, G. P.; Meyer, M. S.; Balogh, M. P.; Kundrat, M. D. *J. Phys. Chem. B* **2005**, *109*, 6.
(23) Filinchuk, Y. E.; Yvon, K.; Meisner, G. P.; Pinkerton, F. E.; Balogh, M. P. *Inorg. Chem.* **2006**, *45*, 1433. Chater, P. A.; David, W. I. F.; Johnson, S. R.; Edwards, P. P.; Anderson, P. A. *Chem. Commun.* **2006**, *23*, 2439.
(24) Cerenius, Y.; Ståhl, K.; Svensson, L. A.; Ursby, T. Oskarsson, Å.; Albertsson, J.; Lijas, A. *J. Synchrotron Radiat.* **2000**, *7*, 203−208.
(25) Hastings, J. B.; Suortii, P.; Thomsolin, P.; Kvick, A.; Koetzle, T. *Nucl. Instrum. Methods* **1983**, *208*, 55.
(26) Clausen, B. S.; Steffensen, G.; Fabius, B.; Villadsen, J.; Feidenhans'l, R.; Topsøe, H. *J. Catal.* **1991**, *132*, 524−535.
(27) Rodriguez, J. A.; Hanson, J. C.; Frenkel, A. I.; Kim, J. Y.; Perez, M. *J. Am. Chem. Soc.* **2002**, *124*, 346.
(28) Hammersley, A. P. Internal Report ESRF-97-HA02T, 1997.
(29) Wong-Ng, W.; McMurdie, H. F.; Paretzkin, B.; Kuchinski, M. A.; Dragoo, A. L. *Powder Diffr.* **1988**, *3*, 247.
(30) Bogdanovic, B.; Schwickardi, M. *J. Alloys Compd.* **1997**, *253*, 1−9.
(31) Au, M.; Jurgensen, A. *J. Phys. Chem. B* **2006**, *110*, 7062−7067.
(32) Hartman, M. R.; Rush, J. J.; Udovic, T. J.; Bowman, R. C., Jr.; Hwang, S.-J. *J. Solid State Chem.* **2007**, *180*, 1298−1305.
(33) Gomes, S.; Hagemann, H.; Yvon, K. *J. Alloys Compd.* **2002**, *346*, 206−210.
(34) Hagemann, H.; Gomes, S.; Renaudin, G.; Yvon, K. *J. Alloys Compd.* **2004**, *363*, 126−129.
(35) Au, M.; Jurgensen, A.; Zeigler, K. *J. Phys. Chem. B* **2006**, *110*, 26482−26487.
(36) Lopez, N.; Janssens, T. V. W.; Clausen, B. S.; Xu, Y.; Mavrikakis, M.; Bligaard, T.; Nørskov, J. K. *J. Catal.* **2004**, *223*, 232−235.
(37) Dutta, B. N.; Dayal, B. *Phys. Status Solidi* **1963**, *3*, 473.
(38) Kienast, G.; Verma, J. *Z. Anorg. Allg. Chem.* **1961**, *310*, 143.